Mineralogical Magazine, October 2009, Vol. 73(5), pp. 871–881

Daliranite, $PbHgAs_2S_6$, a new sulphosalt from the Zarshouran Au-As deposit, Takab region, Iran

W. H. Paar[1,*], A. Pring[2,3], Y. Moëlo[4], C. J. Stanley[5], H. Putz[1], D. Topa[1], A. C. Roberts[6] and R. S. W. Braithwaite[7]

[1] Department of Materials Engineering and Physics (Division of Mineralogy), University of Salzburg, Hellbrunnerstrasse 34, A-5020 Salzburg, Austria
[2] Department of Mineralogy, South Australian Museum, North Terrace, Adelaide, South Australia 5000, Australia
[3] The School of Earth and Environmental Sciences, University of Adelaide, Adelaide, South Australia 5005, Australia
[4] Institut des Matériaux J. Rouxel (IMN), Université de Nantes, CNRS, 2 rue de la Houssinière, F-44322 Nantes Cedex 3, France
[5] The Natural History Museum, Cromwell Road, London SW7 5BD, England, UK
[6] Geological Survey of Canada, 601 Booth Street, Ottawa, Ontario K1A OE8, Canada
[7] School of Chemistry, University of Manchester, Manchester M13 9PL, UK

[*Received 2 June 2009; Accepted 24 August 2009*]

ABSTRACT

Daliranite, ideally $PbHgAs_2S_6$, occurs as a rare sulphosalt species at the Carlin-type Zarshouran Au-As deposit North of the town of Takab in the Province of West Azarbaijan, Iran. The new species is associated with orpiment, rarely with galkhaite, hutchinsonite and cinnabar. The strongly silicified matrix of the specimens has veinlets of sphalerite, with rare inclusions of galena and various (Cu)-Pb-As(Sb) sulphosalts. Daliranite occurs as matted nests of acicular and flexible fibres up to 200 μm in length and a width less than a few μm. The colour is orange-red with a pale orange-red streak and the lustre is adamantine. The mineral is transparent and does not fluoresce. The Mohs hardness is <2. Electron microprobe analyses give the empirical formula $Pb_{0.95}Tl_{0.01}Hg_{1.04}As_{2.10}S_{5.91}$, ideally $PbHgAs_2S_6$; the calculated density is 5.93 g cm^{-3}. Unit-cell parameters were determined by an electron-diffraction study and refined from X-ray powder data. Daliranite is monoclinic primitive with a = 19.113(5) Å, b = 4.233(2) Å, c = 22.958(8) Å, β = 114.78(5)º, V = 1686.4 Å^3 and Z = 8, a:b:c = 4.515:1:5.424, space group $P2$, Pm or $P2/m$. The strongest X-ray powder-diffraction lines [d in Å, (I), (hkl)] are: 8.676, (80), (200); 4.654, (50), ($\bar{4}01$); 3.870, (40), ($\bar{2}11$); 3.394, (50), (113); 3.148, (40b), ($\bar{6}02$); 2.892, (50), ($\bar{6}00$); 2.724, (100), ($\bar{7}03$); 2.185, (50), ($\bar{3}19$). The formula shows a sulphur excess which may correspond to S−S bonding (persulphide). The new sulphosalt is a late phase in the crystallization sequence, and was formed after orpiment, contemporaneously with quartz II, at a temperature between 157 and 193ºC. The name honours Dr Farahnaz Daliran (University of Karlsruhe, Germany) in recognition of her outstanding contributions to research on ore deposits, especially Au, Zn and Fe, in Iran.

Keywords: daliranite, sulphosalt, lead, mercury, arsenic, Zarshouran deposit, West Azarbaijan province, Iran.

Introduction

In 2003, the senior author received several ore samples from Dr Farahnaz Daliran that she had collected at Zarshouran, a significant Au-As deposit in northwest Iran. The sampling was undertaken within the framework of a project funded by the German Scientific Community (DFG-Deutsche Forschungsgemeinschaft) over the period 1998 to 2002.

The bulk of the samples consists of orpiment, frequently in perfectly formed and aesthetically arranged crystals up to 1 cm in size. Almost all

* E-mail: werner.paar@sbg.ac.at
DOI: 10.1180/minmag.2009.073.5.871

samples show a coverage of vibrant orange-red mats of daliranite which strongly resembles ludlockite, $Fe_4PbAs_{10}O_{22}$, described from Tsumeb, Namibia.

Daliranite was probably observed as early as 1971–72 by Dr H.-J. Wilke, a German mineral dealer and collector of rare minerals, who frequently travelled to Iran, and visited the Zarshouran deposit. At that time, daliranite was quite common and occurred in spectacular and very rich samples in cavities of the associated orpiment (Dr H.-J. Wilke, pers. comm. 2008). In his report to the senior author, Dr Wilke pointed out that he had collected a few specimens with daliranite sprays up to a length of several centimetres, associated with quartz and stibnite. This material was later investigated mineralogically, but who did the studies, and which methods were used, remains unclear. More recently however, material collected in the early 1970s was offered for sale by mineral dealers (Germany and the USA) and labelled as 'ludlockite'. Two specimens from this early find, and having this labelling, are registered under # 5726 and # 7676 within the collection of Dr E. Lopatka (Eichberg, Austria). They were acquired by him from Dr H.-J. Wilke, and were identified as daliranite during this study.

A search for additional material during a joint visit of the senior author and Dr Daliran to the Zarshouran deposit in 2005 was unsuccessful. The only mineral collected on the dumps with properties similar to the new species proved to be realgar.

The characterization of this new species was a significant challenge because of the fineness of the hair-like crystals (<3 μm) which caused significant problems for the preparation of suitable polished sections and for the determination of the unit-cell parameters.

The new mineral honours Dr Farahnaz Daliran (born 1953), eminent mineralogist and economic geologist at the University of Karlsruhe (Germany), for her significant contributions to the research of ore deposits in Iran, especially those deposits of Au, Zn and Fe. The new species and its name have been approved by the CNMNC of the IMA (proposal 2007-010). Cotype material (specimens and polished sections – sample numbers 14947 and 14948) is deposited in the Mineralogical Museum of the Department of Materials Engineering and Physics (Mineralogy), University of Salzburg, Austria. A cotype specimen has also been deposited in the collection of the South Australian Museum (G29976). Several specimens containing daliranite are in the collection of Dr F. Daliran. Single specimens have been donated to The Natural History Museum (London), the Landesmuseum Joanneum (Graz, Austria), the mineralogical collection of the University of Halle (Germany) and to the École des Mines of Paris (78986).

The Zarshouran deposit

Zarshouran is a Au-As deposit (36º43.4′ N and 47º08.2′ E) located some 42 km north of the town of Takab in the Province of West Azarbaijan, northwest Iran. The whole Takab District is famous for the ancient mining of As (orpiment and realgar) and alluvial Au, the primary sources of which are very probably epithermal deposits of the Zarshouran or Agdarreh type. To date, indicated reserves of 2.5 Mt of ore averaging 10 ppm Au are estimated. At Agdarreh, the other Au deposit in the region, reserves of 24.5 t Au (measured) and 30–60 t Au at 3.9 ppm (indicated) have been reported (Daliran, 2008; cf. Bariand, 1963).

Zarshouran and Agdarreh (Daliran, 2008) belong to a group of 'SRHDG' deposits (sedimentary-rock-hosted disseminated gold) which are similar to Carlin-type sediment-hosted gold deposits (Daliran *et al.*, 2002; Lescuyer *et al.*, 2003). Both deposits are located within the active geothermal field of the Northern Takab region where thermal springs locally precipitate high amounts of Au and Ag (Daliran, 2003).

At Zarshouran, the mineralization is hosted by metasediments of the basement rocks (schists and marbles) of Upper Proterozoic to Lower Cambrian age which have undergone hydrothermal alteration, including decalcification, dolomitization, sericitization and widespread silicification (formation of jasperoids). Genetically, a relationship to the Tertiary to present-day volcanic-hydrothermal activities within the Urumieh Dokhtar volcanic belt along the convergent plate boundary of Zagros is evident. Geochronological studies by Mehrabi *et al.* (1999) indicate that the Zarshouran deposit was formed at 14.2±0.4 Ma, almost contemporaneously with the volcanic activity (13.7±2.9 Ma). A detailed fluid inclusion study by the same authors revealed a temperature of formation of 243±59ºC at a pressure of 945±445 bar. Daliran *et al.* (1999) and Daliran and Walther (2000) obtained similar temperatures but distinctly lower pressures (~100 bar).

According to Asadi *et al*. (1999, 2000) and Mehrabi *et al*. (1999), three hydrothermal sulphide mineral assemblages have been identified. The early stage includes the formation of pyrrhotite, pyrite and chalcopyrite. Widespread base-metal sulphides, lead sulphosalts (boulangerite, zinkenite, jordanite, geocronite, plagionite, semseyite and twinnite) and zoned arsenical pyrite represent the next stage. The final stage is characterized by abundant arsenical pyrite, sphalerite, coloradoite, and (As, Sb, Hg, Tl)-bearing sulphides and sulphosalts (orpiment, realgar, stibnite, getchellite, galkhaite, hutchinsonite, cinnabar and lorandite).

Native Au is associated with arsenical pyrite and sphalerite. Visible Au of high fineness typically occurs with late-stage orpiment. The highest concentrations of Au were detected in microcrystalline orpiment, carbon-rich shale and silicified shale with pyrite and As-minerals (Asadi *et al*., 2000; F. Daliran, pers. comm. 2005).

Occurrence and paragenesis

The presence of daliranite could not be confirmed within the underground mine at the time of the senior author's last visit. However, the new species must have come from the enormous stocks of cavernous orpiment which are exposed everywhere in the walls of the galleries. In samples collected by Dr F. Daliran in 2000 from the small dumps in front of the only entrance to the mine, daliranite is always associated with orpiment.

Orpiment occurs in particularly well shaped crystals which attain a size of several cm. Typical material shows daliranite (Fig. 1*a*) grown on orpiment and quartz crystals, and rarely accompanied by tiny cubes (<1 mm in size) of galkhaite and prisms of hutchinsonite. Daliranite seems to be a very late phase during crystallization because it always covers orpiment and quartz crystals. Rarely, matted nests of the new species penetrate into orpiment along cracks and fractures, or are included in a late generation of water-clear quartz crystals (Fig. 1*b*).

The strongly silicified matrix of this assemblage contains tiny disseminated crystals of pyrite, irregular veinlets of a chocolate-brown coloured sphalerite, rare grains of cinnabar and microscopic metallic patches which may be composed of galena, members of the bournonite-seligmannite series as well as jordanite, twinnite, a guettardite-like phase and an As-rich variety of zinkenite.

Appearance and physical properties

Daliranite occurs as matted nests of acicular and flexible fibres with a length $\leqslant 200$ μm and a diameter <3 μm. They are elongated parallel to [010]. The colour is a vibrant orange-red, similar to ludlockite, and the streak is pale orange-red. The lustre is adamantine, and the fibres are transparent (Fig. 2). Fluorescence is absent. The Mohs hardness is <2. The thickness of the crystals did not permit a determination of the Vickers microhardness. Cleavage and fracture could not be observed. The density could not be measured

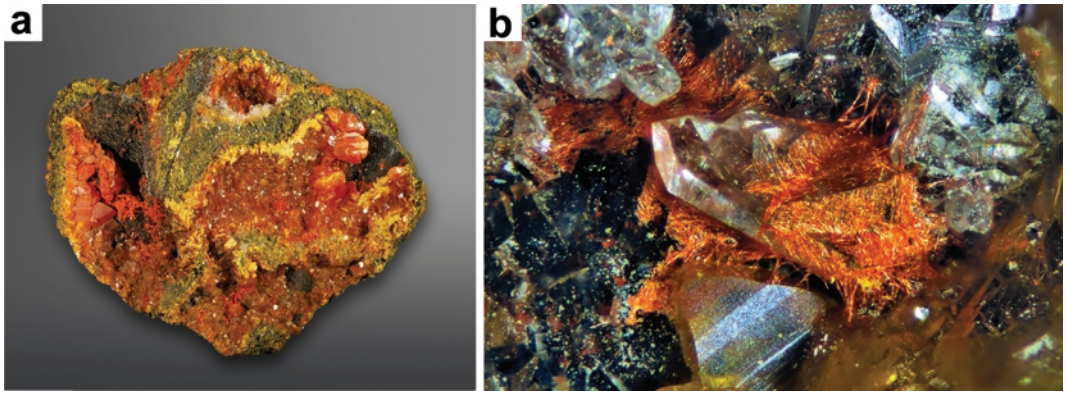

FIG. 1. (*a*) Orange-red nests of fibrous daliranite covering orpiment and quartz; length of specimen = 8 cm. (*b*) Daliranite in orange-red matted nests composed of hair-like crystals, associated with quartz and orpiment crystals. Image width = 3 cm.

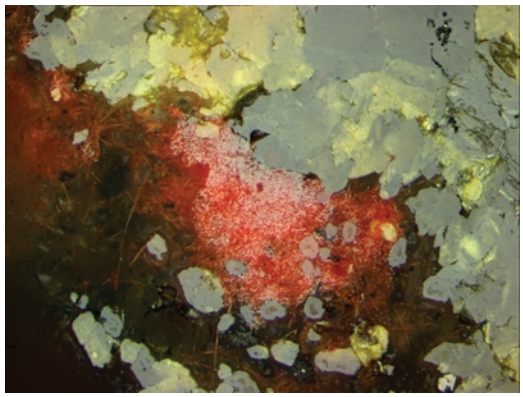

FIG. 2. Reflected-light digital image illustrating daliranite (greyish-white, with red internal reflections) replacing orpiment (yellow internal reflections). PPL (oil immersion). Width of image: 275 μm.

because of admixed quartz, orpiment, sphalerite and cinnabar. Using the empirical formula and the refined unit-cell parameters obtained from the electron-diffraction and powder X-ray diffraction studies, the calculated density, on the basis of the ideal formula, $PbHgAs_2S_6$, is 5.93 g cm^{-3}.

Optical properties

Numerous attempts were made in several laboratories to prepare suitable polished sections in order to measure the optical properties and to determine the quantitative chemistry by electron microprobe analysis. Even when the sample preparation was successful, it was almost impossible to obtain homogeneous areas large enough for the measurements. In almost all cases the 'packing' of the fibres was not dense enough. This resulted in spaces between the fibres which were filled with the embedding resin. Only one single section, carefully prepared by one of the authors (CJS), provided areas with more densely aggregated fibres which allowed us to perform the necessary measurements.

Qualitatively, in incident light, daliranite has a grey colour with a distinctly higher reflectance (5–10%) than that of orpiment (Fig. 2). Pleochroism could not be detected, and the bireflectance is very weak to absent. The anisotropy is always masked by the abundant orange-red internal reflections.

The reflectance values were only determined in air. It was not possible to obtain meaningful measurements in oil. An area of 5 μm × 5 μm, with little or no porosity, was selected. The results are given in Table 1 and Fig. 3, and are the best obtainable on the material available. Orpiment was also measured and matched exactly with orpiment in the QDF (Criddle and Stanley, 1993). We are thus confident of the magnitude of the early *R*′% values for the new species. But, whether the mineral starts to become effectively transparent towards the red end of the spectrum or we are just observing the effects of internal reflections could not be determined.

Chemistry

The infrared spectrum of daliranite was measured in Nujol mull between KBr plates, using a Philips Analytical PU 9600 Fourier Transform infrared spectrometer. Even though a strong mull was employed, no absorptions were detected within the measured range of 400–4000 cm^{-1} apart from those due to the mounting medium. The inference is that O–H, H_2O and oxyanions are absent. Sulphide absorptions are found below

TABLE 1. Reflectance data (R′) and colour values for daliranite.

λ (nm)	*R*′%	Colour values	
400	35.0		
420	34.4	C illuminant	
440	33.8	x	0.318
460	33.2	y	0.310
480	32.6	Y%	32.6
500	32.0	λ_d	~502
520	31.5	Pe%	4.1
540	31.0		
560	31.0		
580	33.0	A illuminant	
600	35.0	x	0.46
620	36.5	y	0.399
640	38.0	Y%	33.2
660	39.0	λ_d	~508
680	38.0	Pe%	5.6
700	37.5		
COM[1]			
470	32.9		
546	30.5		
589	34.0		
650	39.5		

[1] Commission on Ore Mineralogy of the IMA.

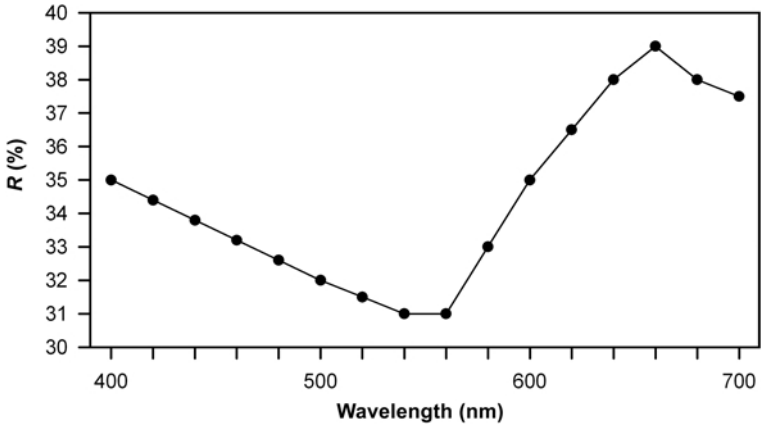

FIG. 3. Reflectance spectrum (in air) of daliranite.

400 cm^{-1} and so were not measureable with the equipment used.

Daliranite was analysed with a JEOL Superprobe JXA-8600, controlled by a LINK-*e***XL** system, operated at 25 kV and 20 nA, at the University of Salzburg. The following natural standards and X-ray lines were used: cinnabar (HgS), Hg-*L*α; galena (PbS), Pb-*M*α; and lorandite ($TlAsS_2$), Tl-*L*α, As-*L*α and S-*K*α. The raw data were corrected with an online ZAF-4 procedure. The results are included in Table 2. No other elements were detected. Lithium, Be and O were sought using ICP-MS techniques, but not observed; Li and Be are <0.01 wt.%. Due to the extreme difficulty in the preparation of the material, the totals of the EMPA are very low due to the presence of epoxy resin between the fibres. Nevertheless, on normalizing all analyses (eight point analyses) to 100%, the atomic proportions almost corresponded exactly to Hg:Pb:As:S = 1:1:2:6. The empirical formula (based on 10 a.p.f.u.) is: $Pb_{0.95}Tl_{0.01}Hg_{1.04}As_{2.10}S_{5.91}$. The simplified formula is $PbHgAs_2S_6$, which requires Pb 27.63, Hg 26.75, As 19.98, S 25.65, total 100.00 wt.%.

Composition of associated sulphosalts

The composition of associated hutchinsonite corresponds to $Tl_{0.98}Pb_{0.95}As_{4.94}S_{9.12}$ (Table 3). Members of the bournonite-seligmannite (Sack and Ebel, 1993; Wu and Birnie, 1977) and jordanite-geocronite solid-solution series are frequently associated with the matrix of the daliranite-bearing orpiment specimens. The As/Sb atomic ratios of the former series vary between 0.09 and 0.5, corresponding to As-rich bournonite, whereas those of the latter are between 1.23 and 1.76, corresponding to Sb-rich jordanite. Traces of Bi (0.14–0.23 wt.%) are detectable in the bournonite.

The chemistry of other sulphosalts closely intergrown with bournonite and/or jordanite is summarized in Table 3. Two samples relate to compounds of the PbS-Sb_2S_3-As_2S_3 system. The composition of the first sample (Z184-1 SS) is intermediate between the dimorph pair twinnite-guettardite (Jambor, 1967) and sartorite, ideally $PbSbAsS_4$ and $PbAs_2S_4$ respectively. This composition is close to $PbAs_{1+x}Sb_{1-x}S_4$, with x ~0.26. The second sample (Z117 SS) has an As/Sb atomic ratio close to 1 (1.13), but the Pb/(Sb+As) atomic ratio (0.40) is too low to correspond to twinnite or guettardite, but is very similar to that of an unnamed As-rich derivative of zinkenite ('mineral AZ') described in the complex sulphide ore deposit of Julcani (Peru) by Duval *et al.* (1986). On the basis of a total of 31 cations, the compositions can be calculated as $Pb_{8.9}Sb_{10.3}As_{11.7}S_{44.2}$ (Zarshouran) and $Ag_{0.4}Pb_{7.7}Sb_{10.9}As_{11.1}Bi_{1.0}S_{41.2}$ (Julcani) respectively.

Two samples, Z184-2 SS and Z184-3 SS, correspond to Cu- and As-bearing zinkenite. According to Moëlo (1983), Cu incorporates in the crystal structure of zinkenite following the heterovalent substitution rule $Sb^{3+} \rightarrow Pb^{2+} + Cu^{+}$. Using the ideal formula $Pb_9Sb_{22}S_{42}$, the two samples of zinkenite have the compositions $Cu_{0.60}Ag_{0.04}Pb_{8.94}Sb_{15.77}As_{6.26}S_{43.65}$ (Z184-SS 2) and $Cu_{0.41}Ag_{0.03}Pb_{8.67}Sb_{21.76}As_{0.54}S_{42.95}$ (Z184-SS 3). The first sample has the highest As content (8.4 wt.%) among occurrences of natural

TABLE 2. Electron microprobe analyses of daliranite.

No.	Pb	Hg	Tl	As	S	Total
1	24.29	25.67	0.18	19.83	23.28	93.26
2	23.82	25.83	0.25	19.81	23.50	93.20
3	24.11	25.52	0.24	19.55	23.45	92.87
4	23.45	25.33	0.19	20.00	23.34	92.31
5	23.07	24.51	0.14	18.17	21.76	87.64
6	22.94	24.47	0.23	17.82	21.70	87.16
7	22.73	23.61	0.17	18.05	21.69	86.26
8	21.70	23.20	0.11	16.75	21.09	82.84
mean	23.26	24.77	0.19	18.75	22.48	89.44
s.d.	0.84	0.98	0.05	1.21	1.00	3.98
Formula (ΣM + S = 10)						
1	0.95	1.04	0.01	2.14	5.87	
2	0.93	1.04	0.01	2.13	5.90	
3	0.94	1.03	0.01	2.11	5.91	
4	0.92	1.02	0.01	2.16	5.89	
5	0.96	1.06	0.01	2.10	5.87	
6	0.96	1.06	0.01	2.07	5.89	
7	0.96	1.03	0.01	2.10	5.91	
8	0.95	1.05	0.01	2.03	5.97	
mean	0.95	1.04	0.01	2.11	5.90	
s.d.	0.02	0.01	0.00	0.04	0.03	

s.d. = standard deviation

zinkenite, which even surpass those in As-rich zinkenite from Jas Roux, French Alps (up to 6.5 wt.%; Mantienne, 1974; Moëlo, 1983). Its As/(Sb+As) atomic ratio (0.28) is very close to the maximum substitution level of 0.30, experimentally obtained at 400ºC by Walia and Chang (1973).

Complex sulphosalts of a similar chemical composition are documented from Agdarreh (Daliran, 2008). Better material, especially larger grains, are needed for an investigation of these minerals by X-ray methods.

Crystallography

Indexed X-ray powder data acquired with a 114.6 mm Debye-Scherrer camera, using Ni-filtered Cu-*K* radiation and based on the primitive monoclinic cell, are presented in Table 4. The data are unique and do not bear a resemblance to any mineral or inorganic compound listed in the Powder Diffraction File up to and including PDF4+ (Release 2008). Single-crystal X-ray precession studies were attempted, but the fibres are too thin to allow diffraction nodes to appear on the films. Electron-diffraction studies were performed using a Philips CM200 TEM. A small matted mass of daliranite fibres was dispersed in a tube of ethanol by immersion for 3 min in an ultrasonic bath. Drops of the ethanol suspension were deposited onto Cu support grids coated with holey carbon films. The daliranite fibres ranged in size from 70 nm up to 200 nm in diameter. The thicker fibres were composed of several intergrown crystals and only the finer fibres gave untwinned diffraction patterns (Fig. 4*a*). Selected-area electron-diffraction (SAED) patterns indicate a primitive monoclinic lattice unit cell approximately 19 Å × 4 Å × 23 Å with β ~115º (Fig 4*b*.) This trail-cell was used to index the powder-diffraction pattern and the unit-cell parameters were refined by least squares methods to give a = 19.113(5) Å, b = 4.233(2) Å, c = 22.958(8) Å, β = 114.78(5)º, V = 1686.4 Å^3, Z = 8, a:b:c = 4.515:1:5.424. Inspection of the SAED patterns and the indexing of the powder cell point to the absence of a 2_1 screw or a c glide so the space group is probably $P2$, Pm or $P2/m$.

TABLE 3. Electron microprobe analyses of sulphosalts associated with daliranite.

No.	Mineral	*n*		Cu	Ag	Pb	Tl	Sb	As	S	Total
1.	Hutchinsonite	10	mean	–	–	18.54	18.97	–	34.90	27.57	99.98
			s.d.			0.21	0.17		0.32	0.14	0.35
2.	Z 184–1 SS	4	mean	0.09	–	38.37	–	17.45	18.45	25.81	100.17
			s.d.	0.03		0.22		0.24	0.27	0.17	0.63
3.	Z 117 SS	2	mean	–	–	34.38	–	23.28	16.29	26.22	100.17
			s.d.			0.30		0.07	0.09	0.02	0.18
4.	Z 184–2 SS	4	mean	0.67	0.08	32.52	–	33.70	8.23	24.57	99.77
			s.d.	0.02	0.05	0.31		0.44	0.26	0.16	0.50
5.	Z 184–3 SS	6	mean	0.43	0.06	30.44	–	44.93	0.68	23.37	99.91
			s.d.	0.04	0.02	0.23		0.48	0.28	0.14	0.46
6.	Jordanite	4	mean	–	–	68.45	–	7.82	6.38	17.86	100.51
			s.d.			0.30		0.30	0.19	0.07	0.14

n = number of analyses
s.d. = standard deviation

Formulae:
1. $Pb_{0.95}Tl_{0.98}As_{4.94}S_{9.13}$
2. $Cu_{0.01}Pb_{0.94}Sb_{0.73}As_{1.25}S_{4.07}$
3. $Pb_{8.9}Sb_{10.3}As_{11.4}S_{44.2}$
4. $Cu_{0.6}Ag_{0.04}Pb_{8.94}Sb_{15.77}As_{6.26}S_{43.65}$
5. $Cu_{0.4}Ag_{0.03}Pb_{8.67}Sb_{21.76}As_{0.54}S_{42.95}$
6. $Pb_{13.71}Sb_{2.67}As_{3.53}S_{23.10}$

Crystal-chemical considerations

Despite the lack of crystal-structure resolution, it is possible to predict some crystal-chemical characteristics of daliranite. Its unit cell has an elongation parameter *a* value close to 4 Å, characteristic of the majority of Pb sulphosalts, whose crystal structures are directly derived from the PbS or SnS archetypes (Makovicky, 1985, 1993). The relatively high value of this elongation

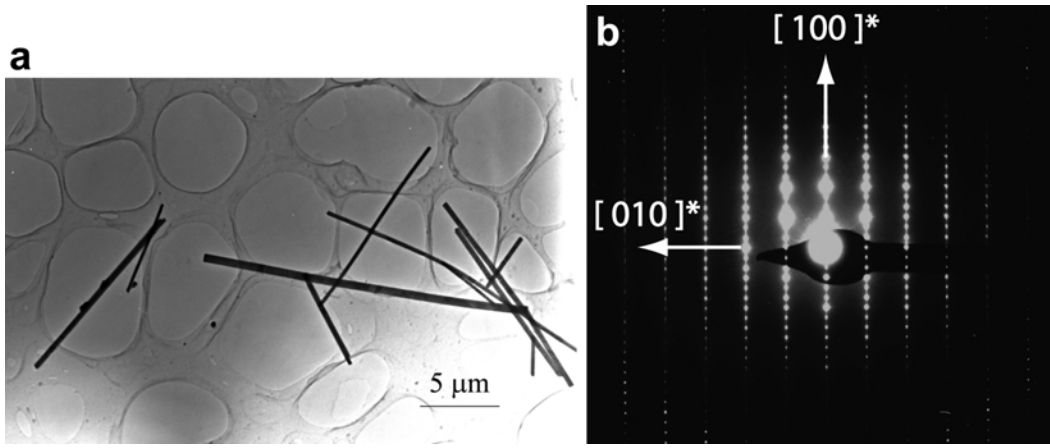

FIG. 4. (*a*) Bright-field electron micrograph showing the size and morphology of the daliranite fibres. (*b*) Electron-diffraction (SAED) pattern of daliranite down the [001] zone with the *a** vertical and *b** running horizontally.

TABLE 4. X-ray powder-diffraction data for daliranite. – 114.6 mm Debye-Scherrer powder camera; Cu-*K* radiation, Ni-filter (λ Cu-*K*α = 1.54178 Å). Intensities visually estimated. Not corrected for shrinkage, and no internal standard.

I/I_o	$d_{obs.}$ (Å)	$d_{calc.}$ (Å)	*h k l*
5	10.43	10.42	0 0 2
80	**8.67**	**8.68**	**2 0 0**
10	7.08	7.06	$\bar{2}$ 0 3
30	5.68	5.68	1 0 3
50	**4.65**	**4.65**	**$\bar{4}$ 0 1**
30	4.34	4.34	4 0 0
10	4.11	4.11	1 1 0
30	3.94	3.94	$\bar{4}$ 0 5
40	**3.87**	**3.87**	**$\bar{2}$ 1 1**
25	3.63	3.63	$\bar{2}$ 1 3
		3.63	2 1 1
20	3.53	3.53	$\bar{4}$ 0 6
		3.40	$\bar{1}$ 1 4
50	**3.40**	**3.39**	**1 1 3**
30	3.31	3.29	0 1 4
40 br	**3.15**	**3.15**	**$\bar{6}$ 0 2**
		3.15	$\bar{4}$ 0 7
25	3.04	3.03	$\bar{4}$ 1 4
		2.899	$\bar{6}$ 0 6
50	**2.894**	**2.892**	**$\bar{6}$ 0 0**
		2.838	$\bar{2}$ 1 6
25	2.833	2.834	2 1 4
		2.831	$\bar{5}$ 1 3
100	**2.722**	**2.724**	**$\bar{7}$ 0 3**
5	2.605	2.605	0 0 8
30	2.530	2.527	$\bar{6}$ 1 4
		2.525	$\bar{4}$ 1 7
5	2.414	2.416	5 1 2
10	2.359	2.359	2 1 6
		2.356	$\bar{7}$ 0 8
10	2.321	2.327	$\bar{8}$ 0 2
5	2.281	2.284	4 0 6
5	2.257	2.257	$\bar{8}$ 0 1
20	2.246	2.249	2 0 8
		2.244	5 0 5
50	**2.187**	**2.185**	**$\bar{3}$ 1 9**
20	2.121	2.122	5 1 4
		2.121	$\bar{9}$ 0 5
10	2.112	2.110	$\bar{1}$ 1 9
10 br	2.070	2.070	$\bar{8}$ 1 3
10	2.041	2.041	$\bar{8}$ 1 6
10	1.998	1.998	$\bar{9}$ 0 1
5	1.974	1.972	10 0 1
		1.933	$\bar{9}$ 0 9
20	1.932	1.932	6 1 4
2	1.910	1.911	$\overline{10}$ 0 5

parameter (4.233 Å) is similar to those of the Pb-As sulphosalts of the sartorite homologous series (Makovicky, 1985; Pring, 2001), but daliranite does not belong to this series, which is characterized by another common intra-layer parameter close to 7.9 Å.

The unit formula shows an excess of S relative to Pb^{2+}, Hg^{2+} and As^{3+}, which may indicate either S–S bonding, or one As^{5+} together with one As^{3+}. In sulphides, As^{5+} presents a tetrahedral coordination with S atoms, with edge lengths close to the ideal value of 3.55 Å. This value does not match the elongation periodicity of daliranite, and it can be concluded that the S excess of daliranite probably corresponds to S–S bonding. Such bonding is known in two natural sulphosalts, as $(S_2)^{2-}$ in livingstonite, $HgSb_4S_6(S_2)$ (Niizeki and Buerger, 1957; Srikrishnan and Nowacki, 1975), or as $(S_3)^{2-}$ in moëloite, $Pb_6Sb_6S_{13}(S_3)$ (Orlandi *et al*., 2002). The disulphide ion is bound to Sb atoms in livingstonite, while $(S_3)^{2-}$ is bound to Pb atoms in moëloite. Other polysulphide complexes are possible; for instance, Hg complexes like $[Hg(S_4)_2]^{2-}$ and $[Hg(S_6)^2]^{2-}$ are known within an organic matrix (Bailey *et al.*, 1991).

In sulphosalt systematics (Moëlo *et al.*, 2008), daliranite constitutes the 18th mineral species in which Hg acts as a specific chemical constituent, and the 5th Pb-Hg sulphosalt, together with marrucciite, mazzettiite, petrovicite and rouxelite. Like livingstonite and moëloite, the excess S permits us to describe daliranite as a persulphide.

Conditions of formation

In the parent material a preliminary study of the fluid inclusions was performed to estimate the conditions of formation of daliranite and the associated phases (Paar and Putz, 2008). For this purpose a Linkam heating-freezing stage equipped with a ×40 universal stage objective was used. For data processing, the software *LinkSys 2.23*, and for the calibration of the system, various standards of *SYNFLINC* were applied. The results are presented in Fig. 5.

Primary fluid inclusions in sphalerite, which is a common constitutent within the matrix of orpiment-daliranite, reveal temperatures of homogenization (T_h) between 191.5 and 236.2ºC, and salinities ranging between 22.4 and 22.7 wt.% NaCl equiv. Supposedly primary inclusions in orpiment which crystallized later than the sphalerite matrix, yielded temperatures of homogenization between 192.8 and 203ºC, and

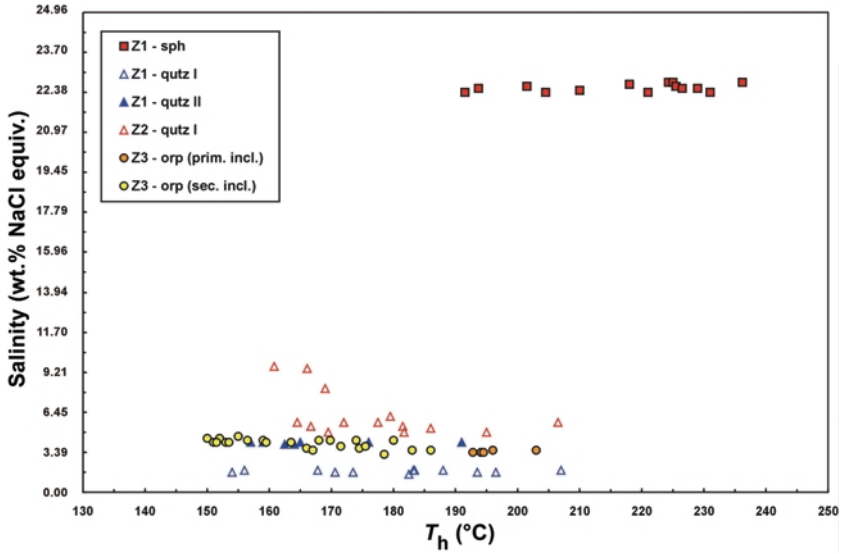

FIG. 5. Salinity/T_h-plot of microthermometric data derived from fluid inclusions of sphalerite, quartz and orpiment from Zarshouran.

secondary inclusions of the same mineral between 150 and 186ºC (3.24–4.65 wt.% NaCl equiv.).

Daliranite is a late phase in the crystallization sequence, and was formed after orpiment, but contemporaneously with quartz II at a temperature between 157 and 193ºC. The relatively low salinity of these fluids (4.0–4.2 wt.% NaCl equiv.) could explain the lack of chloro-sulphides like corderoite, $Hg_3S_2Cl_2$.

The formation of daliranite can be envisaged as a by-product of the reaction of a (Pb,Hg)-bearing fluid with pre-existing orpiment. The fluid may have originated from remobilization of galena and cinnabar which are ubiquitous components of the matrix. Dissolution of orpiment in neutral to basic conditions may favour an increase of sulphur activity, and thus the formation of Hg-polysulphide complexes (Tossell, 1999; Jay *et al.*, 2000; Paquette and Helz, 1997). Such Hg complexes in solution may be the precursors of polysulphide anions probably present within the crystal structure of daliranite.

Acknowledgements

The authors thank the Austrian Academy of Sciences (Kommission für Grundlagen der Mineralrohstoffforschung) for supporting a project which made a study of Au-As deposits in Iran possible. We are very grateful to all colleagues who contributed to the characterization of this very complicated new mineral species: Mag. Dr Peter Spindler (BPFZ-Seibersdorf, Austria) for analytical work (ICP-MS, ICP-OES, AAS); Dr Jochen Schlüter (University of Hamburg) for EMPA; Dr Mark A. Cooper (University of Manitoba) for his attempts to obtain single-crystal cell parameters; Dr Robin Pritchard for attempts at single crystal and synchrotron radiation XRD and Mr Merfyn Jones for powder X-ray diffraction (both at the School of Chemistry, University of Manchester); and Mr D.A. Plant (School of Earth, Atmosphere and Environmental Sciences, University of Manchester) for attempted EMPA, element distribution maps and photos. The reviews by Prof. N. Mozgova and Dr Y. Matsushita as well as the editorial advice of Dr M. Welch helped to improve the content of the paper. We also thank Ing. Norbert Urban (Bad Reichenhall, Germany) for the specimen photos.

References

Asadi, H.H., Voncken, J.H.L. and Hale, M. (1999) Invisible gold at Zarshuran. *Economic Geology*, **94**, 1367–1374.

Asadi, H.H., Voncken, J.H.L., Kühnel, R.A. and Hale, M. (2000) Petrography, mineralogy and geochemistry of the Zarshuran Carlin-like gold deposit, northwest Iran. *Mineralium Deposita*, **35**, 656–671.

Bailey, T.D., Banda, R.M.H., Craig, D.C., Dance, I.G.,

Ma, I.N.L. and Scudder, M.L. (1991) Mercury polysulfide complexes, $[Hg(S_x)_y]^{2-}$: syntheses, mercury-199 NMR studies in solution, and crystal structure of $(Ph_4P)_4[Hg(S_4)_2]Br_2$. *Inorganic Chemistry*, **30**, 187–191.

Bariand, P. (1963) Contribution à la minéralogie de l'Iran. *Bulletin de la Societé française de Minéralogie et de Cristallographie*, **86**, 17–64.

Criddle, A.J. and Stanley, C.J. (1993) *The Quantitative Data File for Ore Minerals (3rd edition)*. The Commission on Ore Mineralogy, International Mineralogical Association. Chapman and Hall, London.

Daliran, F. (2003) Discovery of 1.1 kg/t gold and 2 kg/t silver in mud precipitates of a cold spring from the Takab geothermal field, NW-Iran. Pp. 461–464 in: *Mineral Exploration and Sustainable Development* (D.G. Eliopoulos *et al*., editors). Millpress, Rotterdam, The Netherlands.

Daliran, F. (2008) The carbonate rock-hosted epithermal gold deposit of Agdarreh, Takab geothermal field, Iran – hydrothermal alteration and mineralisation. *Mineralium Deposita*, **43**, 383–404.

Daliran, F. and Walther, J. (2000) A comparative study of the sediment-hosted gold deposits of Agdarreh and Zarshuran at N-Takab geothermal field, NW-Iran. Part II: fluid inclusion study. *European Journal of Mineralogy*, Beihefte **12**, 32.

Daliran, F., Walther, J. and Stüben, D. (1999) Sediment-hosted disseminated gold mineralization in the North-Takab geothermal field. Pp. 837–840 in: *Proceedings of Joint SGA-IAGOD International Meeting*, London.

Daliran, F., Hofstra, A.H., Walther, J. and Stüben, D. (2002) Agdarreh and Zarshuran SRHDG deposits, Takab Region, NW-Iran. *Proceedings of the GSA Annual meeting*, Paper 63-8.

Duval, B., Moëlo, Y. and Picot, P. (1986) Mise en évidence d'un dérivé de la zinkénite, riche en arsenic et bismuth, associé à orpiment, sartorite antimonifère et zinkénite (gisement de Julcani, Pérou). *Bulletin de la Société française de Minéralogie et de Cristallographie*, **109**, 649–655.

Jambor, J.L. (1967) New lead sulfantimonides from Madoc, Ontario. Part 2 – Mineral descriptions. *The Canadian Mineralogist*, **9**, 191–213.

Jay, J.A., Morel, F.M.M. and Hemond, H.F. (2000) Mercury Speciation in the Presence of Polysulfides. *Environmental Science and Technology*, **34**, 2196–2200.

Lescuyer, J.L., Hushmand Zadeh, A. and Daliran, F. (2003) Gold Metallogeny in Iran: a preliminary review. Pp. 1185–1188 in: *Mineral Exploration and Sustainable Development* (D.G. Eliopoulos *et al*., editors), Millpress, Rotterdam, The Netherlands.

Makovicky, E. (1985) The building principles and classification of sulphosalts based on the SnS archetype. *Fortschritte Mineralogie*, **63**, 45–89.

Makovicky, E. (1993) Rod-based sulphosalt structures derived from the SnS and PbS archetypes. *European Journal of Mineralogy*, **5**, 545–591.

Mantienne, J. (1974) *La minéralisation thallifère de Jas-Roux (Hautes-Alpes).* Thesis, University of Paris, 153 pp.

Mehrabi, B., Yardley, G. and Cann, J.R. (1999) Sediment-hosted disseminated gold mineralisation at Zarshuran, NW-Iran. *Mineralium Deposita*, **34**, 673–696.

Moëlo, Y. (1983) *Contribution a l'étude des conditions naturelles de formation des sulfures complexes d'antimoine et plomb*. Document series, **57**, BRGM, Orléans, France, 624 pp.

Moëlo, Y., Makovicky, E., Mozgova, N.N., Jambor, J.L., Cook, N., Pring, A., Paar, W.H., Nickel, E.H., Graeser, S., Karup-Møller, S., Balić-Žunić, T., Mumme, W.G., Vurro, F., Topa, D., Bindi, L., Bente, K. and Shimizu, M. (2008) Sulfosalt systematics: a review. Report of the sulfosalt subcommitee of the IMA Commission on Ore Mineralogy. *European Journal of Mineralogy*, **20**, 7–46.

Niizeki, N. and Buerger, M.J. (1957) The crystal structure of livingstonite, $HgSb_4S_8$. *Zeitschrift für Kristallographie*, **109**, 129–157.

Orlandi, P., Meerschaut, A., Palvadeau, P. and Merlino, S. (2002) Lead-antimony sulfosalts from Tuscany (Italy). V. Definition and crystal structure of moëloite, $Pb_6Sb_6S_{14}(S_3)$, a new mineral from the Ceragiola marble quarry. *European Journal of Mineralogy*, **14**, 599–606.

Paar, W.H. and Putz, H. (2008) *Endbericht zum Teilprojekt 'Epithermale Goldvererzungen in der Takab-Region NW-Iran'*. Austrian Academy of Sciences (ÖAW; Kommission für Grundlagen der Mineralrohstoffforschung). Unpublished report, 16 pp.

Paquette, K.E. and Helz, G.R. (1997) Inorganic speciation of mercury in sulfidic waters: the importance of zero-valent sulfur. *Environmental Science and Technology*, **31**, 2148–2153.

Pring, A. (2001) The crystal chemistry of the sartorite group of minerals from Lengenbach, Binntal. Switzerland: A HRTEM study. *Schweizerische Mineralogische und Petrographische Mitteilungen*, **81**, 69–87.

Sack, R.O. and Ebel, D.S. (1993) As-Sb exchange energies in tetrahedrite-tennantite fahlores and bournonite-seligmannite solid solutions. *Mineralogical Magazine*, **57**, 635–642.

Srikrishnan, T. and Nowacki, W. (1975) A redetermination of the crystal structure of livingstonite, $HgSb_4S_8$. *Zeitschrift für Kristallographie*, **141**, 174–192.

Tossell, J.A. (1999) Theoretical studies on the formation of mercury complexes in solution and the dissolution and reactions of cinnabar. *American Mineralogist*, **84**, 877–883.

Walia, D.S. and Chang, L.L.Y. (1973) Investigations in the systems PbS-Sb_2S_3-As_2S_3 and PbS-Bi_2S_3-As_2S_3. *The Canadian Mineralogist*, **12**, 113–119.

Wu, I.J. and Birnie, R.W. (1977) The bournonite-seligmannite solid solution. *American Mineralogist*, **62**, 1097–1100.